Study on the structure of exotic states $\chi_{c1}(3872)$ via beauty-hadron decays in pp collisions at $\sqrt{s} = 8$ TeV

Chun-tai Wu,[1] Zhi-Lei She,[2] Xin-Ye Peng,[1,*] Xiao-Lin Kang,[1] Hong-Ge Xu,[1] Dai-Mei Zhou,[3] Gang Chen,[1] and Ben-Hao Sa[4]

[1]School of Mathematics and Physics, China University of Geosciences, Wuhan 430074, China
[2]School of Mathematical and Physical Sciences, Wuhan Textile University, Wuhan 430200, China
[3]Key Laboratory of Quark and Lepton Physics, Central China Normal University, Wuhan 430079, China
[4]China Institute of Atomic Energy, P.O. Box 275(10), Beijing 102413, China

(Received 7 March 2023; accepted 1 June 2023; published 15 June 2023)

A dynamically constrained phase-space coalescence (DCPC) model was introduced to study the exotic state $\chi_{c1}(3872)$ yield for three possible structures: tetraquark state, nuclearlike state, and molecular state respectively, where the hadronic final states generated by the parton and hadron cascade model (PACIAE). The $\chi_{c1}(3872)/\psi(2S)$ cross-section ratio from beauty-hadron decays (nonprompt) based on the $\chi_{c1}(3872)$ or $\psi(2S) \to J/\psi\pi^+\pi^-$ bound state in the decay chains as a function of charged-particle multiplicity and transverse momentum in pp collisions at $\sqrt{s} = 8$ TeV are calculated. A tetraquark state scenario from PACIAE+DCPC model shows better agreement with the LHCb and ATLAS measurements for the nonprompt $\chi_{c1}(3872)/\psi(2S)$ cross-section ratio distributions, indicating that the $\chi_{c1}(3872)$ is more likely to be a compact tetraquark state.

DOI: 10.1103/PhysRevD.107.114022

I. INTRODUCTION

In addition to mesons composed of quark-antiquark pairs and baryons consisting of three quarks, many bound states that are incompatible with traditional hadron frameworks have been observed in the decades since the quark model proposed by Gell-Mann in 1964 [1]. These bound states, also known as exotic states, including multiquark states [2–4], hadron molecular states [5], hybrid states [6,7], and glueballs [8], are allowed and expected by the quantum chromodynamics (QCD) and the quark model. While many unconventional hadron candidates containing heavy quarks have been discovered experimentally in recent years [9], the exact nature of even the most well-studied $\chi_{c1}(3872)$ particle, also known as X(3872), is still unclear.

The $\chi_{c1}(3872)$ particle as an exotic charmonium state was observed in the exclusive decay process $B^{\pm} \to K^{\pm}J/\psi\pi^+\pi^-$ by the Belle collaboration in 2003, which decays into $J/\psi\pi^+\pi^-$ [10]. Later, CDF II, D0, BESIII, and *BABAR* collaborations confirmed this exotic state's discovery experimentally [11–14]. Among them, the CDF collaboration proposed that the quantum number of the $\chi_{c1}(3872)$ particle may be $J^{PC} = 1^{++}$ or 2^{-+} [15], and the D0 collaboration suggested that the $\psi(2S)$ state and the $\chi_{c1}(3872)$ state with the same decay mode have the same production and decay properties, which can provide a good benchmark for studying the properties of the $\chi_{c1}(3872)$ particle [12]. Finally, the spin and parity of the $\chi_{c1}(3872)$ state are determined by the LHCb collaboration to $J^{PC} = 1^{++}$ [16]. Although there are several measurements on the $\chi_{c1}(3872)$ particle, due to the lack of the understanding of its exact properties, various models have emerged to describe the $\chi_{c1}(3872)$ state as a $D^{*0}\bar{D}^0$ molecular state with small binding energy [17,18], a compact tetraquark state [19,20], a hybrid meson [21,22], or a charmonium molecule [23,24].

Recently, the prompt $\chi_{c1}(3872)/\psi(2S)$ cross-section ratio was measured at midrapidity by the CMS collaboration as a function of transverse momentum (p_T) in Pb-Pb collisions at $\sqrt{s_{NN}} = 5$ TeV [25]. The central value for the ratio is close to unity and enhanced with respect to the one measured in pp collisions [26,27]. This provides a unique experimental input to theoretical models understanding the $\chi_{c1}(3872)$ production mechanism and the nature of its state since the modification of the hadronization mechanism is predicted when a color-deconfined state of the matter called quark-gluon plasma is formatted in heavy-ion collisions. The a multiphase transport model transport model [28] with instantaneous coalescence, the TAMU model [29] considering only the regeneration processes, and the statistical hadronization model (SHM) [30] based on the assumption

*xinye.peng@cern.ch

of thermal equilibrium predict the different magnitude of the ratio with different scenarios of the structure.

In high-multiplicity pp collisions at LHC energies, the charged-particle densities can reach values comparable with those measured in peripheral heavy-ion collisions. Measurements at such a condition in pp collisions showed features that resemble those in heavy-ion collisions [31–33]. Recently, a multiplicity dependence of the p_{T}-differential $\Lambda_{\mathrm{c}}^{+}/\mathrm{D}^{0}$ ratio is observed by the ALICE collaboration, evolving from pp to Pb-Pb collisions smoothly [34,35]. The prompt $\chi_{c1}(3872)/\psi(2S)$ cross-section ratio is found to decrease as charged-particle multiplicity increases by the LHCb collaboration [36], which is well described by the comover interaction model [37]. The $\chi_{c1}(3872)/\psi(2S)$ cross-section ratio from beauty-hadron decays (nonprompt) showed a slight increase trend as charged-particle multiplicity increases; no theoretical calculation is available for such measurement. Thus, studies about nonprompt $\chi_{c1}(3872)$ production at high multiplicity pp collisions can provide further insight into beauty-quark hadronization as well as an understanding of the nature of the $\chi_{c1}(3872)$ structure.

In this paper, the $\chi_{c1}(3872)$ from beauty-hadron decays, produced in high multiplicity pp collisions at $\sqrt{s} = 8$ TeV, were studied using the Monte Carlo (MC) simulation approach [38]. The multiparticle final states of J/ψ, π^{+} and π^{-} are generated by the parton and hadron cascade (PACIAE) model [39]. The properties of $\chi_{c1}(3872)$ with the hadronic molecular state, the nuclearlike states, or the compact tetraquarks scenario are studied separately using the dynamically constrained phase space coalescence (DCPC) model on these bases [40–45]. With the PACIAE+DCPC model, the nonprompt $\chi_{c1}(3872)$ of three structures to $\psi(2S)$ cross-section ratio as a function of charged particle multiplicity and as a function of p_{T} were predicted. Note that, although different quantum numbers between $\chi_{c1}(3872)$ and $\psi(2S)$ may have influences on this analysis [46], it was not considered in the PACIAE+DCPC model as the measurement is insensitive to such an effect based on Ref. [47].

II. THE PACIAE AND DCPC MODEL

The PACIAE [39] model based on the PYTHIA6.4 [38] is a parton and hadron cascade model that can describe multiple relativistic nuclear collisions. It has been successfully used to describe the particle multiplicity, p_{T}, and rapidity distributions in high-energy collisions [40,45,48–50]. In this paper, the PACIAE model is used to simulate pp collisions, which divides the entire collision process into four main stages: parton initiation, parton rescattering, hadronization, and hadron rescattering.

The initial-state free parton is produced by breaking the strings of quarks, antiquarks, and gluons formed in the pp collision with the PACIAE model. The parton rescattering is further considered using the $2 \to 2$ leading-order (LO) perturbative QCD parton-parton cross sections [51]. The total and differential cross section in the evolution of the deconfined quark matter state is calculated using the MC method. After the partonic freeze-out, the hadronization of the partonic matter is executed by the LUND string fragmentation [38] or the MC coalescence model [39]. Finally, hadron rescattering is performed based on the two-body collision until the hadronic freeze-out.

The hadron yields are calculated based on a two-step approach. First, the multiplicity final states are simulated by the PACIAE model in pp collisions [39]. After that, a transport model (DCPC) is introduced for the calculation of the hadron yields. The details are explained as follows.

From quantum statistical mechanics [52], both position $\vec{q} \equiv (x, y, z)$ and momentum $\vec{p} \equiv (p_x, p_y, p_z)$ of a particle cannot be defined precisely in the six-dimensional phase space, due to the uncertainty principle, $\Delta\vec{q}\Delta\vec{p} \geq h^3$. However, a volume element h^3 in the six-dimensional phase space corresponds to a state of the particle. Thus, the following integral equation can be used to estimate the yield of a single particle:

$$Y_1 = \int_{E_\alpha \leq H \leq E_\beta} \frac{d\vec{q}d\vec{p}}{h^3}, \tag{1}$$

where E_α, E_β, and H are the particle's lower and upper energy thresholds and the Hamiltonian quantity, i.e. the energy function, respectively. Furthermore, the yield of N-particle clusters or bound-state hadrons can be obtained by the following integral equation:

$$Y_N = \int \cdots \int_{E_\alpha \leq H \leq E_\beta} \frac{d\vec{q}_1 d\vec{p}_1 \cdots d\vec{q}_N d\vec{p}_N}{h^{3N}}. \tag{2}$$

For instance, the yield of the $\chi_{c1}(3872)$ particle consisting of J/ψ, π^{+}, and π^{-} can be calculated according to the DCPC model using the following integral formula:

$$Y_{\chi_{c1}(3872)} = \int \cdots \int \delta_{123} \frac{d\vec{q}_1 d\vec{p}_1 d\vec{q}_2 d\vec{p}_2 d\vec{q}_3 d\vec{p}_3}{h^9}, \tag{3}$$

$$\delta_{123} = \begin{cases} 1 & \text{if } 1 \equiv \pi^{+}, 2 \equiv \pi^{-}, 3 \equiv J/\psi; m_0 - \Delta m \leq m_{\mathrm{inv}} \leq m_0 + \Delta m; \mathrm{Max}\{|\vec{q}_{12}|, |\vec{q}_{23}|, |\vec{q}_{31}|\} \leq R_0; \\ 0 & \text{otherwise.} \end{cases} \tag{4}$$

$$m_{\rm inv} = \left[(E_1 + E_2 + E_3)^2 - (\vec{p}_1 + \vec{p}_2 + \vec{p}_3)^2\right]^{\frac{1}{2}}. \quad (5)$$

In Eq. (4), $m_0 = m_{\chi_{c1}(3872)} = 3871.69\ \mathrm{MeV/c^2}$ represents the rest mass of the $\chi_{c1}(3872)$ particle [53], R_0 stands for its radius and Δm denotes the uncertainty of the mass. $|\vec{q}_{12}|$, $|\vec{q}_{23}|$, and $|\vec{q}_{31}|$ indicate the distances between each of the three component particles π^+, π^- and J/ψ under the center-of-mass system, respectively, while $\mathrm{Max}\{|\vec{q}_{12}|, |\vec{q}_{23}|, |\vec{q}_{31}|\}$ represents the maximum distance taken between them. The Hamiltonian quantity H satisfies the equation $H^2 = (\vec{p}_{J/\psi} + \vec{p}_{\pi^+} + \vec{p}_{\pi^-})^2 + m_{\rm inv}^2$, and the energy threshold upper and lower limits E_α and E_β satisfy $E_{\alpha,\beta} = (\vec{p}_{J/\psi} + \vec{p}_{\pi^+} + \vec{p}_{\pi^-})^2 + (m_{\chi_{c1}(3872)} \mp \Delta m)^2$. Thus the dynamic constraint condition $E_\alpha \le H \le E_\beta$ in Eq. (1) can be equivalently replaced by $m_{\chi_{c1}(3872)} - \Delta m \le m_{\rm inv} \le m_{\chi_{c1}(3872)} + \Delta m$ in Eq. (4).

III. RESULTS

The final-state hadrons, including J/ψ, π^+, and π^-, are simulated using the PACIAE model in pp collision at $\sqrt{s} = 7$ TeV. All of the parameters are fixed to the default values in the PACIAE model, except parj(1), parj(2), and parj(3), which are determined by fitting data from the LHCb collaboration for J/ψ, π^+, and π^- in pp collisions at $\sqrt{s} = 7$ TeV. Here, parj(1), parj(2), and parj(3) factors are related to the suppression of diquark-antidiquark pair production compared with quark-antiquark production, the suppression of s quark pair production compared with u or d pair production, and the extra suppression of strange diquark production compared with the normal suppression of strange quark, respectively. With the configurations of $\mathrm{parj}(1) = 0.10$, $\mathrm{parj}(2) = 0.20$, and $\mathrm{parj}(3) = 0.90$, the production of J/ψ, π^+, and π^- generated by the PACIAE model fits the ALICE and LHCb data [54,55] well. Table I summarizes the comparison of the nonprompt J/ψ, π^+, and π^- integrated yields at the same $p_{\rm T}$ and rapidity coverage between experimental data and the PACIAE model.

Assuming no dependence of PACIAE model parameters between $\sqrt{s} = 7$ and 8 TeV, the simulation was redone at 8 TeV. After that, the exotic state $\chi_{c1}(3872)$ is constructed by the combination of J/ψ, π^+, and π^- using the DCPC model. Half of the $\chi_{c1}(3872)$ decay width is used as the Δm parameter, i.e, $\Delta m = \Gamma/2 = 1.95$ MeV [45,56]. The $\chi_{c1}(3872)$ can be separated into three possible structures according to $\mathrm{Max}\{|\vec{q}_{12}|, |\vec{q}_{23}|, |\vec{q}_{31}|\}$. The tetraquark state, the nuclearlike state, and the molecular state are defined with the radius interval $R_0 < 1.2$ fm (χ_{c1}^t) [57], $1.2 < R_0 < 1.96$ fm (χ_{c1}^n) [58], and $1.96 < R_0 < 10$ fm (χ_{c1}^m), respectively.

Figure 1 shows the nonprompt $\chi_{c1}(3872)/\psi(2S)$ cross-section ratios in the $J/\psi\pi^+\pi^-$ decay channels with three structures χ_{c1}^t, χ_{c1}^n, and χ_{c1}^m in pp collisions at $\sqrt{s} = 8$ TeV, as a function of charged-particle multiplicity (N_{ch}). Here, the $\psi(2S)$ yields are calculated in the same way as $\chi_{c1}(3872)$ described above. The N_{ch} represents the number of charged particles at the $2 < y < 5$ rapidity interval to match the LHCb data [36]. The nonprompt $\chi_{c1}^t/\psi(2S)$ cross-section ratio is consistent with the LHCb data within uncertainties [36], while other scenarios show larger deviation with respect to the data, indicating that $\chi_{c1}(3872)$ is more likely to be a compact quark state. Both of these three scenarios show a similar flat trend with the increasing of the N_{ch} within uncertainties, consistent with the data measurement. From the PACIAE+DCPC model, the number of nonprompt $\chi_{c1}(3872)$ naturally increases with the increasing of the multiplicity, similar to $\psi(2S)$ [3]. Note that the increasing of multiplicity will also lead to a more significant final-state effect of $\chi_{c1}(3872)$ destruction by the comoving particles in the PACIAE+DCPC model, resulting in a decrease of the $\chi_{c1}(3872)$ yields [37,59,60]. Similarly, $\psi(2S)$ yields are also suppressed by the final-state breakup interaction of the quarkonium with the comoving particles. However, the same as argued in

TABLE I. The J/ψ, π^+ and π^- yields in pp collisions at $\sqrt{s} = 7$ TeV calculated by the PACIAE model, compared to the ALICE and LHCb data [54,55] in $|y| < 0.5, 0.1 < p_T < 3$ GeV/c for $\pi^\pm$ and $2 < y < 4.5, 0 < p_T < 14$ GeV/c for nonprompt J/ψ, respectively.

Particle	ALICE or LHCb data [54,55]	PACIAE
J/ψ	$(1.60 \pm 0.01 \pm 0.23) \times 10^{-5}$	$(1.60 \pm 0.03) \times 10^{-5}$
π^+	2.26 ± 0.10	2.26 ± 0.01
π^-	2.23 ± 0.10	2.25 ± 0.03

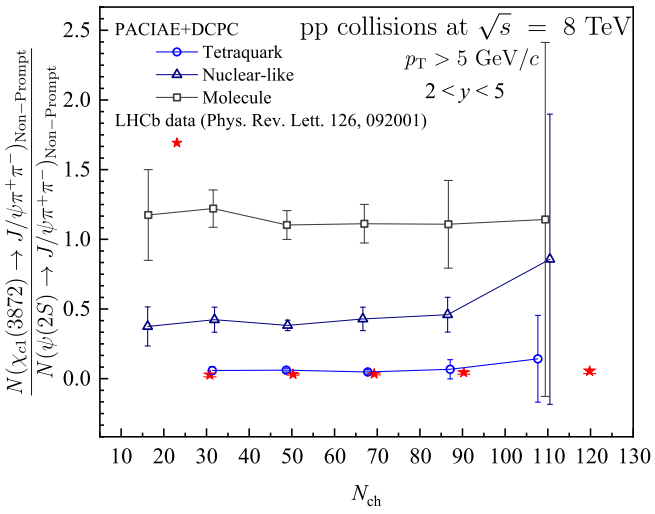

FIG. 1. The nonprompt $\chi_{c1}(3872)$ to $\psi(2S)$ cross-section ratios in the $J/\psi\pi^+\pi^-$ decay channels obtained with three structures χ_{c1}^t, χ_{c1}^n, and χ_{c1}^m in pp collisions at $\sqrt{s} = 8$ TeV, as a function of charged-particle multiplicity. The open points are computed using the PACIAE+DCPC model, and the solid red points are from the LHCb data [36].

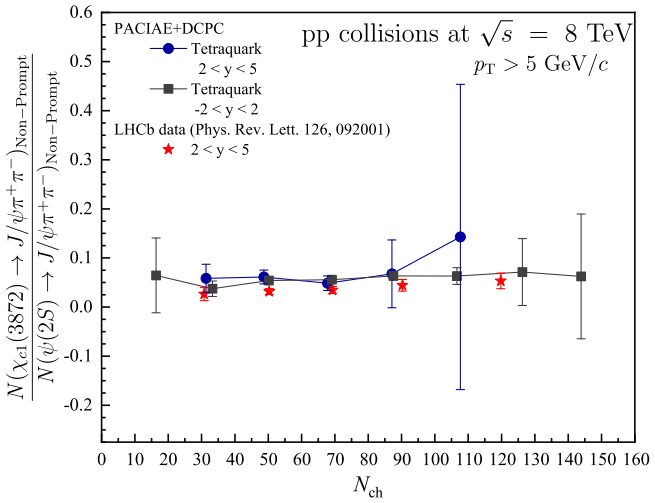

FIG. 2. The comparison of the nonprompt $\chi_{c1}(3872)/\psi(2S)$ cross-section ratio as a function of charged-particle multiplicity at middle $(-2 < y < 2)$ and forward rapidity $(2 < y < 5)$ from the PACIAE+DCPC model, compared to the LHCb data at forward rapidity [36]. The blue and black points represent the PACIAE+DCPC model results in middle and forward rapidity, respectively, and the solid red points are from the LHCb data at forward rapidity [36].

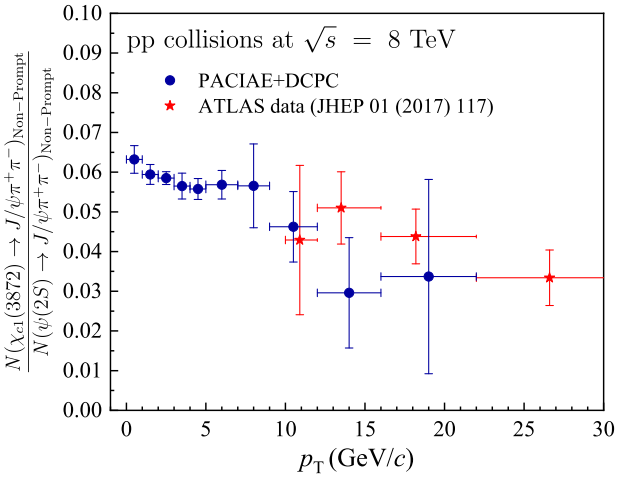

FIG. 3. The nonprompt $\chi_{c1}(3872)/\psi(2S)$ cross-section ratio as a function of p_T in pp collisions obtained with the PACIAE+DCPC model at $\sqrt{s} = 8$ TeV, compared with the ATLAS data [26].

Ref. [36], the effect is less pronounced for nonprompt $\chi_{c1}(3872)$ and $\psi(2S)$ since they are produced from displaced beauty-hadron decay vertices, where the particle density is largely reduced with respect to the primary vertex.

The PACIAE+DCPC model predicts different magnitude for the nonprompt $\chi_{c1}(3872)/\psi(2S)$ cross-section ratio based on different structures, with the hierarchy $\chi^t_{c1} < \chi^n_{c1} < \chi^m_{c1}$. From the PACIAE+DCPC model, it is harder to generate the nonprompt χ^t_{c1} with tetraquark structure with respect to other scenarios since the radius interval for the tetraquark state is smaller; it is more difficult to form the nonprompt χ^t_{c1} in the limited phase space via the coalescence mechanism.

A natural next step would be to study the properties of $\chi_{c1}(3872)$ as a compact tetraquark state, as the rapidity and p_T dependence of the nonprompt $\chi_{c1}(3872)/\psi(2S)$ cross-section ratio may give further insight into beauty-quark hadronization. Figure 2 reports the nonprompt $\chi_{c1}(3872)/\psi(2S)$ cross-section ratio with tetraquark scenario as a function of charged-particle multiplicity at middle rapidity $(-2 < y < 2)$ and forward rapidity $(2 < y < 5)$, compared to the LHCb data at forward rapidity [36]. The results from the PACIAE+DCPC model indicate minor rapidity dependence for the nonprompt $\chi_{c1}(3872)/\psi(2S)$ cross-section ratio.

The nonprompt $\chi_{c1}(3872)/\psi(2S)$ cross-section ratio with tetraquark scenario as a function of p_T at middle rapidity is presented in Fig. 3. The result is compared with the ATLAS measurement [26]. In the common interval $10 < p_T < 22$ GeV/c, the result from the PACIAE+DCPC model shows a good agreement with the ATLAS data within uncertainties. The model result predicts a slightly increasing trend toward low p_T, mainly due to the larger coalescence probability for $\chi_{c1}(3872)$ at the low p_T region. Nevertheless, the decay kinematic effect may also play a role due to the mass difference between the parent-beauty hadron and nonprompt hadron for these two particles [61], which is hard to isolate for such nonprompt hadron measurements.

IV. CONCLUSIONS

In summary, the PACIAE model is used to generate final-state particles in pp collisions at $\sqrt{s} = 8$ TeV. The π^+, π^-, and J/ψ originating from beauty-hadron decays are inserted into the DCPC model to produce the exotic state $\chi_{c1}(3872)$. With different spatial parameters R_0 selected, the exotic states $\chi_{c1}(3872)$ of three different structures are constructed as compact tetraquark state, nuclearlike state, and molecular state, respectively. The nonprompt $\chi_{c1}(3872)/\psi(2S)$ cross-section ratios in the $J/\psi\pi^+\pi^-$ decay channels with the three structures as a function of charged-particle multiplicity are obtained from the PACIAE+DCPC model; the compact tetraquark state scenario describes the LHCb data well, indicating that the $\chi_{c1}(3872)$ is more likely to be a compact quark state. Meanwhile, the PACIAE+DCPC model predicts a minor rapidity dependence and a decreasing trend with the increasing of the p_T for the ratio, indicating that the coalescence mechanism may play an important role in the beauty-quark hadronization in a small system. In particular, the slightly decreasing trend with the increasing of the p_T for the nonprompt $\chi_{c1}(3872)/\psi(2S)$ cross-section ratio predicted by the PACIAE+DCPC model at low p_T, can be further tested with the ongoing high luminosity run 3 data at the LHC by multiexperiments.

ACKNOWLEDGMENTS

The work of X. Y. Peng is supported by the NSFC Key Grant No. 12061141008 and the National key research and development program of China under No. 2018YFE0104800, the National Natural Science Foundation of China (NSFC) (Grant No. 12205259), and the work of X. L. Kang is supported by the NSFC (No. 12005195).

[1] M. Gell-Mann, Phys. Lett. **8**, 214 (1964).
[2] R. L. Jaffe, Phys. Rev. D **15**, 267 (1977).
[3] J. Matthew Durham (LHCb Collaboration), Nucl. Phys. **A1005**, 121918 (2021).
[4] S. Dubnicka, A. Z. Dubnickova, M. A. Ivanov, and J. G. Korner, Phys. Rev. D **81**, 114007 (2010).
[5] M. T. AlFiky, F. Gabbiani, and A. A. Petrov, Phys. Lett. B **640**, 238 (2006).
[6] F. E. Close and P. R. Page, Nucl. Phys. **B443**, 233 (1995).
[7] R. L. Jaffe, Phys. Rev. Lett. **38**, 195 (1977); **38**, 617(E) (1977).
[8] K. K. Seth, Phys. Lett. B **612**, 1 (2005).
[9] S. L. Olsen, T. Skwarnicki, and D. Zieminska, Rev. Mod. Phys. **90**, 015003 (2018).
[10] S. K. Choi *et al.* (Belle Collaboration), Phys. Rev. Lett. **91**, 262001 (2003).
[11] D. Acosta *et al.* (CDF Collaboration), Phys. Rev. Lett. **93**, 072001 (2004).
[12] V. M. Abazov *et al.* (D0 Collaboration), Phys. Rev. Lett. **93**, 162002 (2004).
[13] B. Aubert *et al.* (*BABAR* Collaboration), Phys. Rev. D **71**, 071103 (2005).
[14] M. Ablikim *et al.* (BESIII Collaboration), Phys. Rev. Lett. **112**, 092001 (2014).
[15] A. Abulencia *et al.* (CDF Collaboration), Phys. Rev. Lett. **98**, 132002 (2007).
[16] R. Aaij *et al.* (LHCb Collaboration), Phys. Rev. Lett. **110**, 222001 (2013).
[17] E. Braaten and M. Kusunoki, Phys. Rev. D **69**, 074005 (2004).
[18] E. Braaten and M. Kusunoki, Phys. Rev. D **71**, 074005 (2005).
[19] L. Maiani, F. Piccinini, A. D. Polosa, and V. Riquer, Phys. Rev. D **71**, 014028 (2005).
[20] R. D. Matheus, S. Narison, M. Nielsen, and J. M. Richard, Phys. Rev. D **75**, 014005 (2007).
[21] B. A. Li, Phys. Lett. B **605**, 306 (2005).
[22] F. E. Close and S. Godfrey, Phys. Lett. B **574**, 210 (2003).
[23] N. N. Achasov and E. V. Rogozina, Mod. Phys. Lett. A **30**, 1550181 (2015).
[24] R. D. Matheus, F. S. Navarra, M. Nielsen, and C. M. Zanetti, Phys. Rev. D **80**, 056002 (2009).
[25] A. M. Sirunyan *et al.* (CMS Collaboration), Phys. Rev. Lett. **128**, 032001 (2022).
[26] M. Aaboud *et al.* (ATLAS Collaboration), J. High Energy Phys. 01 (2017) 117.
[27] S. Chatrchyan *et al.* (CMS Collaboration), J. High Energy Phys. 04 (2013) 154.
[28] H. Zhang, J. Liao, E. Wang, Q. Wang, and H. Xing, Phys. Rev. Lett. **126**, 012301 (2021).
[29] B. Wu, X. Du, M. Sibila, and R. Rapp, Eur. Phys. J. A **57**, 122 (2021); **57**, 314(E) (2021).
[30] A. Andronic, P. Braun-Munzinger, M. K. Köhler, K. Redlich, and J. Stachel, Phys. Lett. B **797**, 134836 (2019).
[31] V. Khachatryan *et al.* (CMS Collaboration), J. High Energy Phys. 09 (2010) 091.
[32] G. Aad *et al.* (ATLAS Collaboration), Phys. Rev. Lett. **116**, 172301 (2016).
[33] J. Adam *et al.* (ALICE Collaboration), Nat. Phys. **13**, 535 (2017).
[34] S. Acharya *et al.* (ALICE Collaboration), Phys. Lett. B **829**, 137065 (2022).
[35] S. Acharya *et al.* (ALICE Collaboration), Phys. Lett. B **839**, 137796 (2023).
[36] R. Aaij *et al.* (LHCb Collaboration), Phys. Rev. Lett. **126**, 092001 (2021).
[37] A. Esposito, E. G. Ferreiro, A. Pilloni, A. D. Polosa, and C. A. Salgado, Eur. Phys. J. C **81**, 669 (2021).
[38] T. Sjostrand, S. Mrenna, and P. Z. Skands, J. High Energy Phys. 05 (2006) 026.
[39] B.-H. Sa, D.-M. Zhou, Y.-L. Yan, X.-M. Li, S.-Q. Feng, B.-G. Dong, and X. Cai, Comput. Phys. Commun. **183**, 333 (2012).
[40] G. Chen, Y.-L. Yan, D.-S. Li, D.-M. Zhou, M.-J. Wang, B.-G. Dong, and B.-H. Sa, Phys. Rev. C **86**, 054910 (2012).
[41] Y.-L. Yan, G. Chen, X.-M. Li, D.-M. Zhou, M.-J. Wang, S.-Y. Hu, L. Ye, and B.-H. Sa, Phys. Rev. C **85**, 024907 (2012).
[42] G. Chen, H. Chen, J. Wu, D.-S. Li, and M.-J. Wang, Phys. Rev. C **88**, 034908 (2013).
[43] Z. Zhang, L. Zheng, G. Chen, H.-G. Xu, D.-M. Zhou, Y.-L. Yan, and B.-H. Sa, Eur. Phys. J. C **81**, 198 (2021).
[44] C.-h. Chen, Y.-L. Xie, H.-g. Xu, Z. Zhang, D.-M. Zhou, Z.-L. She, and G. Chen, Phys. Rev. D **105**, 054013 (2022).
[45] H.-g. Xu, Z.-L. She, D.-M. Zhou, L. Zheng, X.-L. Kang, G. Chen, and B.-H. Sa, Eur. Phys. J. C **81**, 784 (2021).
[46] N. Barnea, J. Vijande, and A. Valcarce, Phys. Rev. D **73**, 054004 (2006).
[47] F. Carvalho, E. R. Cazaroto, V. P. Gonçalves, and F. S. Navarra, Phys. Rev. D **93**, 034004 (2016).
[48] Y.-L. Yan, B.-G. Dong, D.-M. Zhou, X.-M. Li, and B.-H. Sa, Phys. Lett. B **660**, 478 (2008).
[49] D.-M. Zhou, L. Zheng, Z.-H. Song, Y.-L. Yan, G. Chen, X.-M. Li, X. Cai, and B.-H. Sa, Phys. Rev. C **102**, 044903 (2020).
[50] L. Zheng, D.-M. Zhou, Z.-B. Yin, Y.-L. Yan, G. Chen, X. Cai, and B.-H. Sa, Phys. Rev. C **98**, 034917 (2018).

[51] B. L. Combridge, J. Kripfganz, and J. Ranft, Phys. Lett. **70B**, 234 (1977).
[52] K. Stowe, *An Introduction to Thermodynamics and Statistical Mechanics* (Cambridge University, Cambridge, England, 2007).
[53] M. Tanabashi *et al.* (Particle Data Group Collaboration), Phys. Rev. D **98**, 030001 (2018).
[54] J. Adam *et al.* (ALICE Collaboration), Eur. Phys. J. C **75**, 226 (2015).
[55] R. Aaij *et al.* (LHCb Collaboration), Eur. Phys. J. C **71**, 1645 (2011).
[56] T. Aushev *et al.* (Belle Collaboration), Phys. Rev. D **81**, 031103 (2010).
[57] L. S. Kisslinger, W.-h. Ma, and P. Hoodbhoy, Nucl. Phys. **A459**, 645 (1986).
[58] S. I. Y. Wu and T. Sasakawa, Few-Body Syst. **15**, 145 (1993).
[59] E. G. Ferreiro and J.-P. Lansberg, J. High Energy Phys. 10 (2018) 094; 03 (2019) 63.
[60] E. G. Ferreiro, Phys. Lett. B **749**, 98 (2015).
[61] S. Acharya *et al.* (ALICE Collaboration), J. High Energy Phys. 12 (2022) 126.